THE JOURNAL OF PHYSICAL CHEMISTRY B

ARTICLE

pubs.acs.org/JPCB

Diffusion-Limited Energy Transfer in Blends of Oligofluorenes with an Anthracene Derivative

Rodrigo Q. Albuquerque,*[,†] Christiane C. Hofmann,[‡] Jürgen Köhler,[‡] and Anna Köhler*[,†]

[†]Experimental Physics II, Universität Bayreuth Universitätstrasse 30, 95440 Bayreuth, Germany

[‡]Experimental Physics IV, Universität Bayreuth Universitätstrasse 30, 95440 Bayreuth, Germany

Supporting Information

ABSTRACT: Organic semiconductor devices such as light-emitting diodes and solar cells frequently comprise a blend of molecular or polymeric materials. Consequently, resonant energy transfer between the components plays a major role in determining device performance. Energy transfer may take place through either single-step donor−acceptor transfer, realized for example as Förster transfer, or as a sequence of donor−donor transfers toward the acceptor site. Here we use a well-defined model system comprising an oligofluorene trimer, pentamer, or heptamer as the donor in combination with an anthracene derivative as the acceptor in order to study the rate and mechanism of energy transfer in thin films by time-resolved photoluminescence spectroscopy. We find the transfer process to be entirely dominated by sequential donor−donor transfer. In addition, we observe a strong dependence on oligomer length with an optimum energy transfer rate for the pentamer.

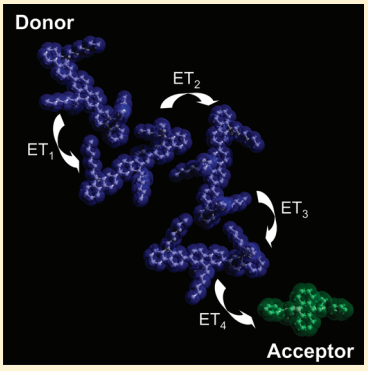

1. INTRODUCTION

Excitation energy transfer is a key process controlling the function of many organic semiconductor devices such as polymer light-emitting diodes (PLEDs) or photovoltaic cells.[1,2] The realization of efficient semiconductor devices often requires the use of several molecular components, among which energy transfer may take place. By using smart device architectures or material combinations, energy transfer can be employed to improve the device performance, be it with respect to luminescence efficiency or emission color, such as white-light emission,[3] polarization of emission,[4] or solar cell efficiency.[2,5] Despite the immense progress made with many optoelectronic applications and despite several studies,[6−15] there are still a number of questions that concern the underlying photophysical processes. One of these issues relates to how energy is transferred within a film of organic semiconductors.[16−18]

There are two modes for how energy can be transferred from a donor chromophore to an acceptor site. One well investigated process consists of a single step resonant energy transfer (RET) from donor to acceptor by the interaction of their transition dipoles. Essential features of this process, such as the long range of the interaction and the dependence on spectral overlap between donor emission and acceptor absorption, have been recognized early, and they were related to experimentally accessible spectroscopic quantities by Förster.[19] His expressions are widely used and highly successful due to their simplicity, though they require the donor and acceptor transition dipoles to be approximated as points (point−dipole approximation (PDA)) which only holds for large donor−acceptor separation. Today, there are a number of quantum chemical approaches available to compute the electronic coupling between donor and acceptor with high accuracy even at short distances.[20−23]

An alternative process of transferring an excitation from a donor to an acceptor is by a sequence of donor−donor energy transfer steps, also referred to as energy migration, followed by a final nearest-neighbor donor−acceptor transfer.[13−15,24] Each transfer will itself be subject to some electronic coupling mediated either by dipole−dipole or exchange interaction. Essentially, the excitation migrates from donor to acceptor through an incoherent hopping process. This kind of exciton diffusion is frequently encountered in dense media, such as molecular crystals or amorphous organic films.

In amorphous films of a donor host doped with a small amount of an acceptor guest, both processes can, in principle, take place, and the resulting energy transfer mechanism is likely to be a superposition of both modes, depending on time and distance after the excitation. For the design of host−guest systems, such as the ones used in solar cell applications, the rate of energy transfer is a critical parameter determining the transfer efficiency and the exciton diffusion length. It is therefore useful to explore whether both modes need to be considered (and thus optimized) or whether it is sufficient to focus on improving the material parameters for only one mode of transfer. Here, we use oligomers as well-defined model systems to investigate how the nature of energy transfer depends on oligomer length and acceptor concentration. We compare energy transfer rates using either an oligofluorene

Received: March 11, 2011
Revised: May 16, 2011
Published: June 02, 2011

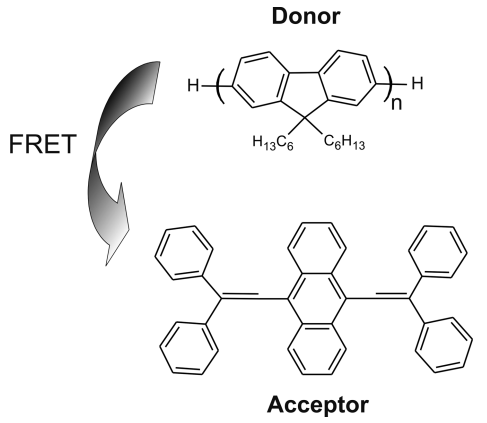

Figure 1. Molecular structures of the oligofluorene trimer D3 (n = 3), pentamer D5 (n = 5), and heptamer D7 (n = 7) used as donors and the anthracene-derivative AD used as an acceptor in the process of fluorescence resonant energy transfer (FRET).

trimer, pentamer, or heptamer as the donor in combination with an anthracene derivative as the acceptor (Figure 1).

2. EXPERIMENTAL SECTION

The oligofluorenes D3, D5, and D7, as well as the anthracene derivative (AD), were purchased from ADS Dyes and used without further purification. Thin films were prepared by spin-coating from chlorobenzene solution in the absence of UV light and then stored in the dark. The film thickness was about 70 nm as measured on a Dektak 150 surface profilometer (Veeco).

Absorption spectra at room temperature were measured on a Varian Cary 5000 double-beam UV/vis/NIR spectrometer and baseline corrected. Steady state emission and excitation spectra were recorded on a fluorimeter LS-50B (Perkin-Elmer), where the films were placed inside a quartz cuvette and flushed with argon.

The lifetimes of the samples spin-coated from chlorobenzene were measured with a time-correlated single photon counting (TCSPC) setup consisting of a FluoTime 200 spectrometer (PicoQuant), a pulsed diode laser (λ = 375 nm, 64 ps fwhm, typical pulse energy 10 pJ, PicoQuant) with a repetition rate of 20 MHz, and a MCP-PMT (multichannel-plate−photon−multiplier-tube) detector. The instrument response function (IRF) for this system is about 70 ps. The emissions were detected with the monochromator set at 415 nm when the oligofluorene decay was recorded or at 500 nm to measure the decay of the anthracene derivative. To obtain a good signal:noise ratio, a slit width of 1 mm was used, implying a spectral resolution of about 20 nm. The films were kept inside a quartz cuvette and flushed with argon before and during the measurements. The low pulse energies employed imply that the fractions of excited donor and acceptor molecules are below 10^{-7} and 10^{-6}, respectively. In our analysis, we can thus neglect any nonlinear effects due to excited acceptor molecules.[18]

To double-check the lifetime measurements, we have also determined the lifetimes of films spun from tetrahydrofurane (THF) using a pulsed titanium:sapphire laser system (Tsunami, Spectra Physics, 1−2 ps fwhm) with λ_{exc} = 355 nm and an excitation energy per pulse of 10^{-12} to 5×10^{-11} J. The emission from the sample was collected with an achromatic lens under right angle conditions. The detection was made using a combination of a spectrograph (250 Imaging Spectrograph, Bruker) and a streak camera (C5680 series, Hamamatsu), giving spectral and temporal resolutions of ca. 3 nm and 3 ps, respectively. The lifetimes were fitted considering the spectral range 406−432 nm and were found consistent with the TCSPC measurements. A more detailed comparison between the lifetimes obtained by TCSPC and by streak camera measurements is given in the Supporting Information.

Emission quantum yields (Φ) were measured by placing the samples inside a N_2 flushed integrating sphere. An argon ion laser (Innova 300C, Coherent) with multiline excitation at λ_{exc} = 351 and 364 nm was used to irradiate the sample. The light emitted was collected through a small hole in the integrating sphere by a glass fiber and detected by a CCD (charge coupled device) camera (Andor Idus) coupled to a spectrograph. The laser power was kept at 1 mW to avoid bleaching of the dyes. Φ was calculated using the method described in ref 25.

For the calculation of R_0 (see eqs 4 and 5), the refraction index of polyfluorene at 3.0 eV was used, that is, n = 2.2.[4] The overlap integral J was calculated using the emission spectra of the prepared donor films spin-coated from chlorobenzene and the absorption spectrum of the acceptor film. Neat thin films of the anthracene derivative are turbid and exhibit a significant amount of scattering, resulting in a red tail of the absorption spectrum (see the Supporting Information). For an accurate calculation of the overlap integral J, we have therefore fitted the absorption spectrum with a single Gaussian peak (see the Supporting Information) and scaled it with the molar absorptivity coefficient.

For the analysis of the results, it is important to know the mean center-to-center distance r between an excited donor and an acceptor. In order to derive this from the acceptor concentration, we adopted a Monte Carlo procedure as follows. We took for the blends a density of 1 g cm^{-3}, which is the density reported for polyfluorene derivatives.[26] This corresponds to the following molecular volumes: V = 1660 Å^3 (D3), 2765 Å^3 (D5), and 3867 Å^3 (D7). The molecular volume of the anthracene derivative was calculated from the measured thickness of the film and its molar absorptivity, giving V = 1355 Å^3. For each molar ratio of donor:acceptor, a computational box with volume given by the sum of the molecular volumes of donors and acceptor was simulated using a Monte Carlo algorithm, in which the positions of the molecular centers of the donors distributed around the acceptor were randomly generated. In this procedure, the minimum center-to-center distance between any two generated molecular centers was 6 Å, estimated based on their van der Waals clouds. Several iterations were used for each single sample of a given donor:acceptor ratio in order to have better statistics. The mean of all donor−acceptor distances generated was then used as the center-to-center distance r. This Monte Carlo approach was found consistent with a rough estimate based on considering both donor and acceptor as spheres and by calculating the mean center-to-center distance between them.

3. RESULTS

The absorption and emission spectra of the oligomer films and the photoluminescence excitation and emission spectra of the anthracene derivative are shown in Figure 2a. For the anthracene derivative, we show the excitation spectrum instead of the absorption spectrum, as the absorption is affected by scattering (see the Supporting Information). For all three oligofluorenes, we observe a good spectral overlap between the emission from the oligofluorene donor and the absorption of the anthracene

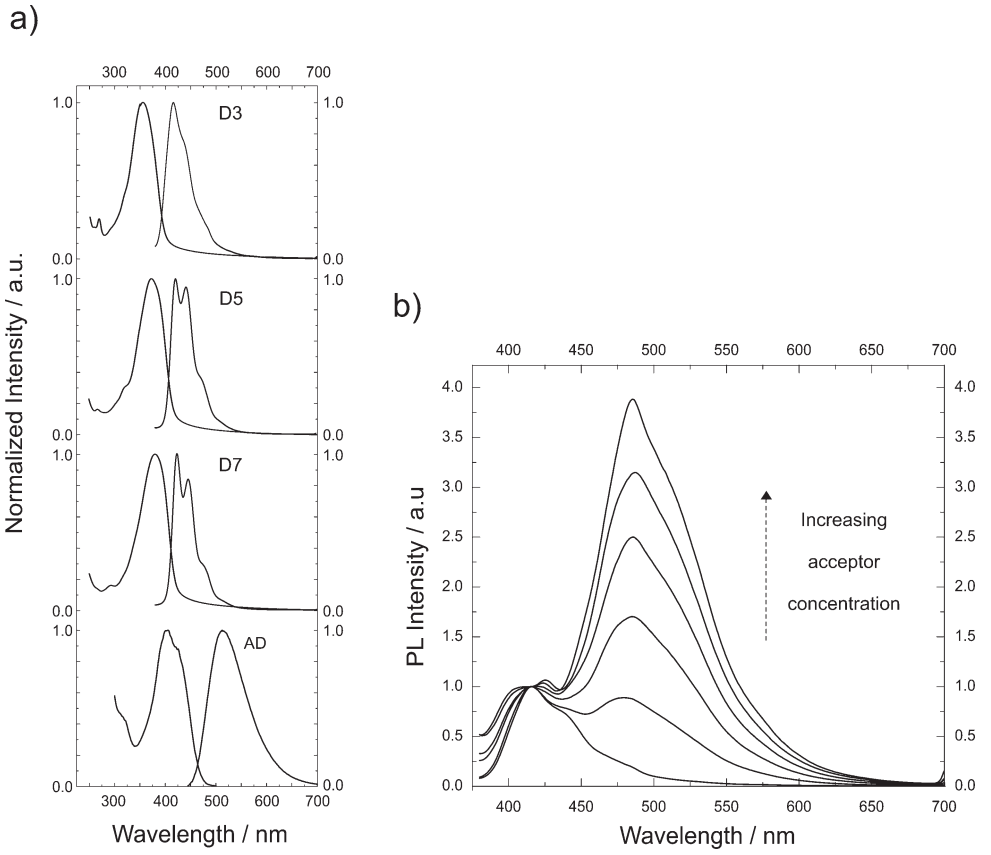

Figure 2. (a) Normalized absorption and emission spectra of neat films of the oligofluorenes and the normalized excitation and emission spectra of the anthracene derivative (AD) at room temperature. (b) Emission spectra of the blends containing different D3:AD ratios (AD content in mol %: 0, 0.5, 1.0, 1.5, 2.0, 2.5) recorded at room temperature under argon atmosphere with λ_{exc} = 355 nm. The spectra were normalized at 415 nm, where the emission of D3 peaks.

acceptor. Thus, in principle, Förster-type energy transfer between the oligofluorene donor and the anthracene derivative acceptor is possible.

Figure 2b shows the emission spectra of thin films made from blends of the fluorene trimer with the anthracene derivative at different donor:acceptor ratios (in mol %) normalized at the emission of the fluorene trimer (λ = 415 nm). When the mol percentage of the anthracene derivative in the blend is raised from 0 up to 2.5%, we observe an intense additional emission band with a peak at 485 nm. This band increases in intensity with anthracene content, and it dominates the spectrum for only 2.5 mol % of anthracene derivative. We attribute this band to emission from the anthracene derivative due to efficient energy transfer from the fluorene trimer. The slight apparent blue-shift of the anthracene derivative emission in the blend compared to the neat film might be caused by some degree of self-absorption in the neat film.

3.1. Experimental Determination of the Energy Transfer Rate. In order to experimentally determine the rate of energy transfer, k_{ET}, we require the time dependence of the photoluminescence of the donor in the absence ($f(t)$) and in the presence ($g(t)$) of the acceptor. The rate equation for the decay of the luminescence in the neat film can be expressed as

$$\frac{d}{dt}f(t) = -\left(\frac{1}{\tau_{0,D}} + k(t)\right)f(t) \qquad (1)$$

where $\tau_{0,D}$ is the natural exciton lifetime of the donor in the absence of acceptor and $k(t)$ represents any further time-dependent decay processes (e.g., exciton diffusion to quenching or annihilation sites) that take place independent of the presence or absence of an acceptor. When the acceptor is added, the donor luminescence decays as

$$\frac{d}{dt}g(t) = -\left(\frac{1}{\tau_{0,D}} + k(t)\right)g(t) - k_{ET}(t)g(t) \qquad (2)$$

where $k_{ET}(t)$ is the rate of energy transfer from donor to acceptor. Combining eqs 1 and 2 leads to an expression for $k_{ET}(t)$ that is independent of $k(t)$:[13]

$$k_{ET}(t) = -\frac{d}{dt}\ln(g(t)/f(t)) \qquad (3)$$

i.e., the energy transfer rate can be determined experimentally when $f(t)$ and $g(t)$ are known. The photoluminescence decay traces for the oligofluorene donors with and without the anthracene derivative acceptor are presented in Figure 3 for all blends at different donor:acceptor molar ratios. The decay from the neat oligofluorenes is monoexponential. When the anthracene derivative is added, we observe a fast initial decay by about 3 decades within roughly 1.5 ns, corresponding to decay times in the range of a few hundred ps, followed by a slower decay with time constants in the range of 2−3 ns. We attribute the fast decay to the oligofluorene emission, while the slower decay is associated

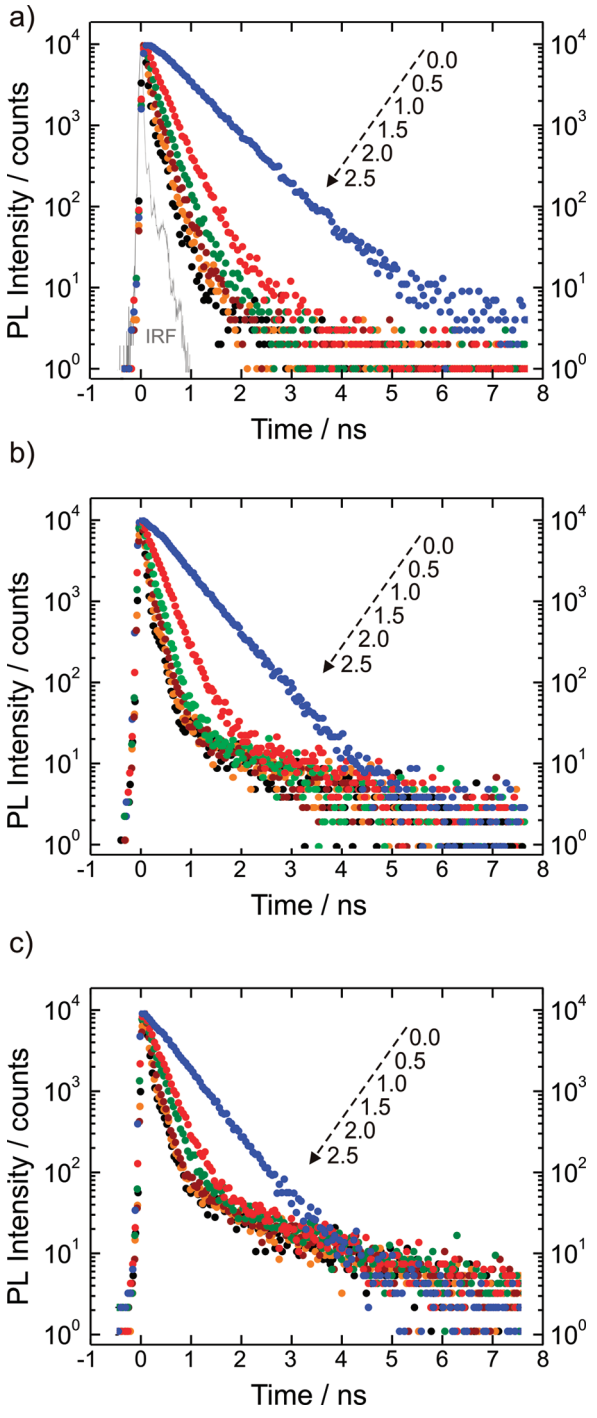

Figure 3. Experimental photoluminescence decays in thin films at room temperature (a) of the blends D3:AD along with the instrument response function (IRF), (b) of the blends D5:AD, and (c) of the blends D7:AD, all with different amounts of acceptor as indicated in the figure in mol %.

with the emission of the anthracene derivative. This is consistent with the fact that the decay of the fast component accelerates with increasing anthracene content, in contrast to the slow component. Furthermore, in a neat film of the anthracene derivative, we determined a lifetime of about 2 ns.

The associated ratio of $g(t)/f(t)$ versus time is shown in Figure 4 for a time range up to 1.5 ns. Within this time window, the contribution from the anthracene derivative emission to the total intensity can be neglected. As expected, we observe steeper slopes, i.e., higher transfer rates, with increasing acceptor concentration. Note that $I(t) = g(t)/f(t)$ represents the surviving exciton population. The lines shown in Figure 4 are stretched-exponential fits of the type $I(t) = I_0 \exp[-(t/\tau)^{\alpha}]$, where I_0 is the intensity at time $t = 0$, α is a parameter that can be related to the dynamics and dimensionality of the excitation transfer,[14,27] and τ is the decay time constant specific for each system. Such streched-exponential functions are characteristic for averages over a distribution of monoexponential decays, as is the case in the ensemble considered here. On average, the blends have exhibited α values of about 0.8 $\pm$ 0.1. The τ values for the oligofluorenes decrease from about 600 ps in the neat films and 400 ps for 0.5% of acceptor down to 100 ps for 2.5% of acceptor. The constants τ and α obtained for all blends are listed in the Supporting Information.

Following eq 3, the energy transfer rate can be derived by evaluating the slope of $\ln((g(t)/f(t))$. Figure 5a shows, for t = 250 ps, how such experimental RET rates vary for the different oligomers as a function of acceptor concentration. The full time dependence of k_{ET} is shown in the Supporting Information for reference, along with the transfer rates and donor−acceptor distances shown in Figure 5. From Figure 5a, we observe two features. First, the energy transfer rates increase approximately linearly with molar concentration, implying an approximately cubic dependence on donor−acceptor distance. Second, the energy transfer rates increase from the trimer to the pentamer but then reduce when going to the heptamer. To get insight into this, one needs to keep in mind that the oligomers vary considerably in length. The approximate lengths of the oligofluorenes are 24 Å (D3), 41 Å (D5), and 57 Å (D7). An appropriate comparison among oligomer RET rates requires displaying this data as a function of mean donor−acceptor separation (center-to-center distance r). This is shown in Figure 5b. As expected, we observe an increase in transfer rates for short center-to-center distances. Further, we see that the energy transfer rates for the pentamer and the heptamer are identical within the experimental error, while the trimer is characterized by a slightly lower energy transfer rate.

3.2. Determination of Energy Transfer Rate Using the Förster Theory. In order to get insight into the mechanism of energy transfer, we want to compare the experimentally derived RET rates with energy transfer rates calculated assuming a single-step donor−acceptor transfer. The most accessible and most convenient line of approach is to use the Förster formalism in the limit of the point-dipole approximation. In the PDA, the electronic coupling between donor and acceptor promoting the energy transfer is considered to be that of two point dipoles. This yields equations that can be evaluated using spectroscopic data, i.e., experimentally available quantities. This is of considerable practical advantage. However, caution needs to be exercised when using the point−dipole approximation, since it has been shown to be a poor approximation for extended π-conjugated chromophores at short donor−acceptor distances.[20] It is therefore necessary to consider the kind of error possibly introduced by employing this approximation. The PDA overestimates the rates of energy transfer for two molecules in cofacial orientation, while it underestimates the rate of head-to-tail transfer.[28] This leads to some cancellation of errors when the energy transfer is isotropically averaged.[29] While the exact magnitude of the relative error depends on the size of the chromophores' transition dipole

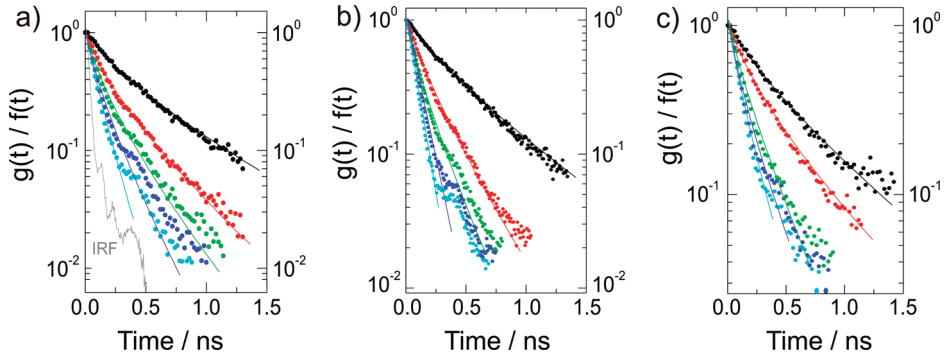

Figure 4. The ratio $g(t)/f(t)$ versus time for the blends (a) D3:AD, (b) D5:AD, and (c) D7:AD with AD content of 0.5 (black dots), 1.0 (red dots), 1.5 (green dots), 2.0 (blue dots), and 2.5 (sky blue dots), all given in mol %. $g(t)$ and $f(t)$ are the donor decays in the presence and in the absence of acceptor, respectively. The instrument response function (IRF) is also shown in this plot (gray line). The lines are stretched-exponential fits corresponding to $I(t) = I_0 \exp(\tau/\tau_0)^{\alpha}$.

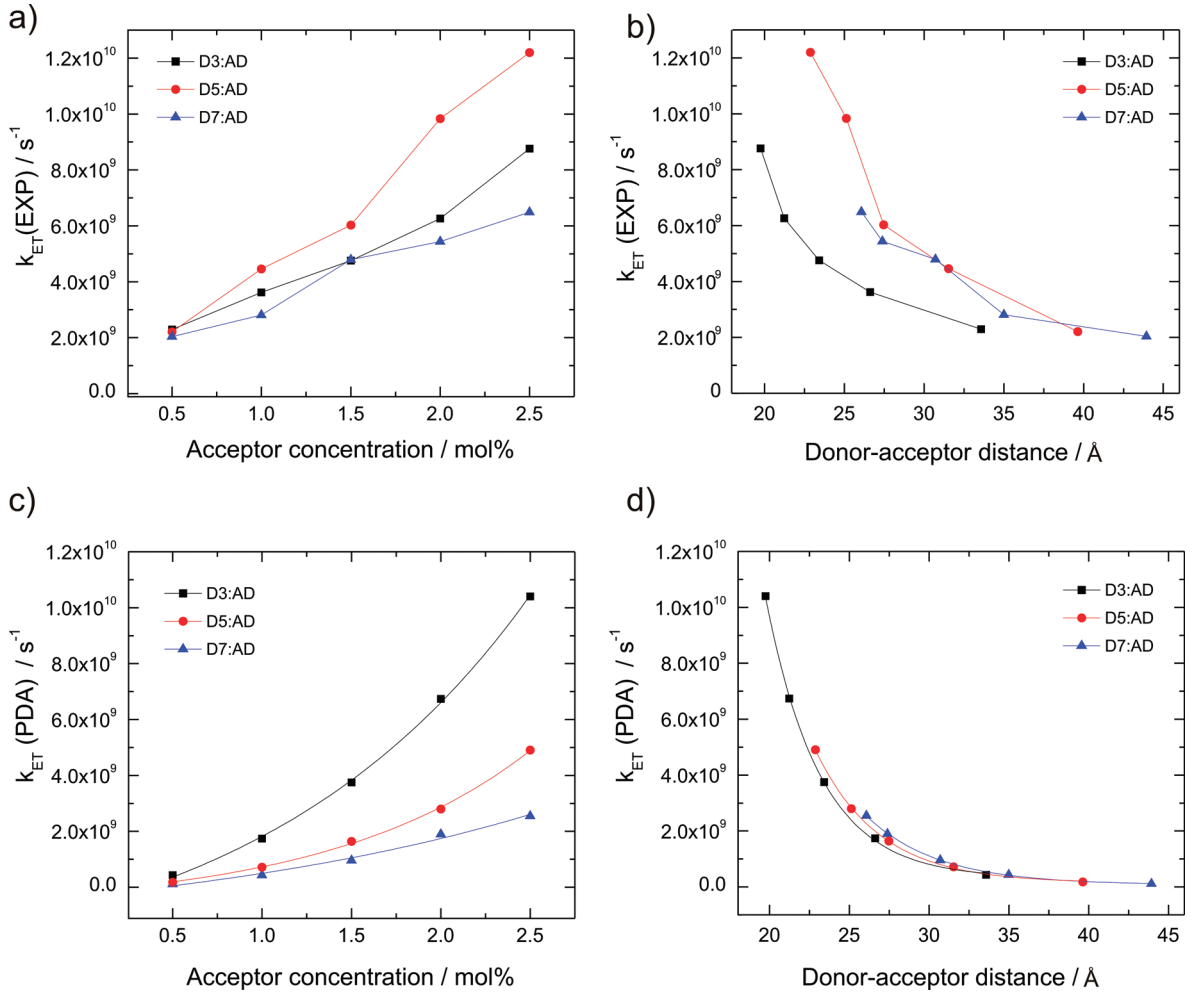

Figure 5. Rates for energy transfer from the oligofluorenes D3, D5, and D7 to the anthracene derivative AD as a function of acceptor concentration and as a function of donor−acceptor center-to-center distance. Parts a and b show the experimental k_{ET}(EXP) values derived by using eq 3 at $t = 250$ ps. Parts c and d show the values, k_{ET}(PDA), expected from the Förster expression (within the point-dipole approximation), eq 4, on the basis of the spectroscopic data. The lines serve only to guide the eye.

moment, there is agreement that serious inaccuracies are in particular introduced for distances below 20 Å.[29,30] In the work presented here, we only consider donor−acceptor distances above 20 Å. In amorphous films, a range of relative orientations is sampled (even though spin-coating may introduce some degree of orientation in a plane), thus reducing the errors introduced by the PDA to some degree. Nevertheless, based on the geometry of the molecules, we consider that there is likely

dx.doi.org/10.1021/jp202333w |J. Phys. Chem. B 2011, 115, 8063–8070

Table 1. The Input Parameters Used to Derive R_0 by eq 5, along with the Resulting R_0 Values for the Donor:Acceptor Blends

donor	J (10^{14} M^{-1} cm^{-1} nm^4)	ε (10^3 M^{-1} cm^{-1})	$\tau_{0,D}$ (ns)	$\Phi_{0,D}$	R_0 (Å)
D3	5.66	85.1	0.67	0.41	27.3
D5	5.46	135.9	0.58	0.42	27.3
D7	5.31	196.8	0.52	0.44	27.4

to be a remaining contribution due to RET between cofacially oriented molecules. Thus, in total, the PDA employed may tend to overestimate the transfer rates somewhat. Keeping this in mind, we now proceed to derive the energy transfer rates expected for a single-step Förster-type donor−acceptor transfer.

According to Förster, the FRET rate from the donor to the acceptor separated from each other by a center-to-center distance r is given by[19]

$$k_{ET} = \frac{1}{\tau_{0,D}}\left(\frac{R_0}{r}\right)^6 \quad (4)$$

where $\tau_{0,D}$ is the lifetime of the donor in the absence of an acceptor and R_0 is called the Förster radius, which corresponds to the distance at which the rate of energy transfer to the acceptor equals all other decay rates of the donor. On the basis of previous work, Förster was able to relate R_0 to quantities that are available by steady-state spectroscopy:

$$R_0\ (\mathrm{nm}) = 0.02108\left(\frac{\kappa^2 \phi_{0,D} J\ (M^{-1}\ cm^{-1}\ nm^4)}{{n_0}^4}\right)^{1/6} \quad (5)$$

where n_0 is the refraction index of the medium, $\phi_{0,D}$ is the emission quantum yield of the donor in the absence of acceptor, J is the overlap integral between the area-normalized emission spectrum of the donor and the absorption spectrum of the acceptor scaled by its molar extinction coefficient, and κ^2 is a spatial factor that describes the relative orientation of the transition dipole moments of donor and acceptor.[31]

We have derived the values for J and $\tau_{0,D}$ from Figures 2 and 3. The emission quantum yield was measured using the integrating sphere method.[25] For n_0, we used the refractive index of polyfluorene at 3.0 eV, that is 2.2 as determined by ellipsometry.[4] For κ^2, we assumed a random, yet fixed isotropic distribution, implying $\kappa^2 = 0.476$, though it needs to be kept in mind that there is likely to be some degree of planar orientation in films prepared by spin-coating.[12] The values used as parameters to put into eqs 4 and 5 are listed in Table 1.

On the basis of the spectroscopic data, we find that all energy transfer pairs should exhibit about the same value for the Förster radius R_0 of 27 Å. Thus, according to eq 4, the energy transfer rate will only vary with donor lifetime and donor−acceptor separation. The energy transfer rates based on eq 4, k_{ET}(PDA), are shown in Figure 5c and d as a function of acceptor concentration and donor−acceptor center-to-center distance. For the same donor:acceptor molar ratio, the energy transfer rate increases from D7 to D3. However, when considering the center-to-center distance, all three oligomers are predicted to give essentially equal transfer rates.

3.3. Comparison between Energy Transfer Rates Derived by Experiment and by Förster Theory. We are now in a position to compare the energy transfer rates obtained from lifetime measurements by using eq 3, k_{ET}(EXP), with the ones we get when using the spectroscopic steady state data as input to the Förster expression eq 4, k_{ET}(PDA). Figure 6 shows how the ratio of k_{ET}(EXP)/k_{ET}(PDA) evolves with center-to-center distance. We find the experimental transfer rates not only exceed the ones predicted by Förster theory, but moreover, this discrepancy *increases* with donor−acceptor distance. The point-dipole approximation used for Förster theory is known to fail at short distances; however, it returns more accurate results at larger separation between donor and acceptor. The increasing discrepancy between experimental rates and rates derived using Förster theory as a function of distance therefore can only be interpreted as a signature of donor−donor transfer as outlined below.

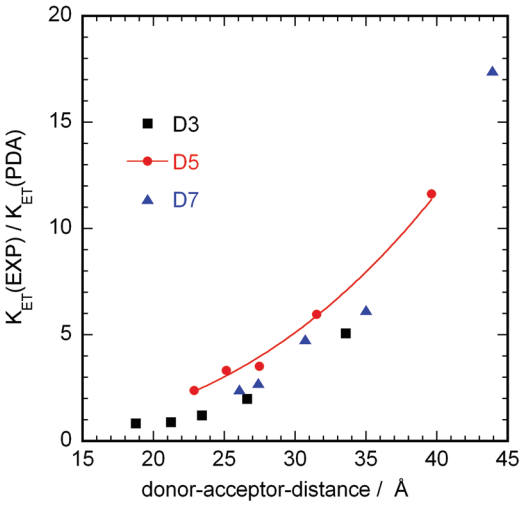

Figure 6. Ratio between k_{ET}(EXP) and k_{ET}(PDA) as a function of donor−acceptor center-to-center distance for blends of the acceptor with D3, D5, and D7. For the D5 blend, the solid line indicates a fit to a $r^{2.9}$ dependence.

4. DISCUSSION

Energy transfer processes between different chromophores play a central role across the disciplines of physics, chemistry, and biology. For example, energy transfer is exploited through smart architecture of semiconductor devices such as organic light emitting diodes,[3] through clever chemical design of chromophore or antennae systems for organic solar cells,[32,33] and it controls the performance of biological phenomena, such as light harvesting processes in bacteria.[34] A thorough and fundamental understanding of parameters that control energy transfer is thus of general interest, and consequently, resonant energy transfer (RET) has been intensely researched.[20]

In this work, we concentrate on the effects of oligomer length on the energy transfer dynamics in thin amorphous films. Thin (70 nm) films of a donor−acceptor blend are frequently employed for organic semiconductor devices. We are interested in two issues. First, we aim to understand by which mechanism energy is transferred from donor to acceptor in a thin film structure. Second, we address whether there is a certain oligomer length that makes this process most efficient. To get insight into the transfer mechanism, let us consider two limiting cases.

(i) We assume all transfer occurs by a single-step Förster process. In this case, the energy transfer rate depends

inversely on the square of the concentration, i.e., $k_{ET}(PDA) \propto r^{-6}$. Further, the time dependence $I(t) = I_0 \exp[-(t/\tau)^{\alpha}]$ of the surviving exciton population $I(t) = g(t)/f(t)$ is given by a coefficient of $\alpha = 0.5$ for three-dimensional energy transfer. In the case of two-dimensional energy transfer, this would reduce to $\alpha = 0.33$.[27]

(ii) Another limiting case is obtained if energy is transferred to the acceptor entirely by a sequence of donor−donor hops (followed by a final nearest neighbor donor−acceptor hop).[9,12,15,24] In this case, the overall energy transfer rate from donor to acceptor, say $k_{ET}(DD)$, depends linearly on the concentration of the acceptor, i.e., $k_{ET}(DD) \propto r^{-3}$. $I(t) = I_0 \exp[-(t/\tau)^{\alpha}]$ is characterized by a coefficient of $\alpha = 1$ if the rate of donor−donor transfer is constant. This can be easily seen when considering the rate equation for the fluorescence intensity I_F

$$\frac{dI_F}{dt} = G - (k_0 + ck_{ET})[S] \quad (6)$$

where G is the generation rate of singlet excitons, k_0 is the sum of the radiative and nonradiative singlet exciton decay rates in the absence of the acceptor, c is the concentration of the acceptor, k_{ET} is the rate of energy transfer from donor to acceptor (mediated by donor−donor hops), and $[S]$ is the concentration of singlet excitons. Solving eq 6 yields a fluorescence lifetime of $\tau_F = (k_0 + ck_{ET})^{-1}$, implying that

$$I_F(t) = I_0 \exp[-(k_0 + ck_{ET})t] \quad (7)$$

i.e., the exponent α is 1 if k_{ET} is independent of time. Donor−donor energy transfer in amorphous films of π-conjugated molecules or polymers proceeds as spectral diffusion in an inhomogeneously broadened density of states.[14,15,24] This diffusion process has been shown to slow down with time in a logarithmic fashion,[35] resulting in a coefficient of α slightly below 1.

Let us now recall our experimental findings. The measurements of the fluorescence lifetime at various acceptor concentrations (Figures 3 and 4) have indicated a value of $\alpha = 0.8 \pm 0.1$, and yield an approximately linear dependence of the energy transfer rate on concentration (Figure 5a), implying that k_{ET} is approximately proportional to r^{-3}. These entirely experimental values are clearly much closer to the scenario of a sequence of donor−donor transfers ($k_{ET}(DD) \propto r^{-3}$) in an inhomogeneously broadened density of states ($\alpha < 1$) than to the predictions for a single-step donor−acceptor transfer ($k_{ET}(PDA) \propto r^{-6}$), even when taking into account possible inaccuracies due to the PDA. Thus, from this comparison, it appears that energy transfer in a thin amorphous film is dominated by sequential donor−donor transfer, and that single-step Förster transfer plays only a minor role.

With this comparatively simple spectroscopic approach, we aim to derive some physical insight into the distance dependence of the energy transfer mechanism. Figure 6 indicates the *difference* between the predicted Förster rate and the experimentally measured rate increases approximately with the cube of the distance, i.e., linear with concentration. Clearly, when the experimental energy transfer is dominated by donor−donor mediated transfer, thus being linearly dependent on acceptor concentration and the Förster rate depends quadratically on concentration, the ratio between the two should also depend linearly on acceptor concentration. Such a linear relationship is evident in Figure 6. This implies that sequential donor−donor transfer, i.e., incoherent exciton migration, dominates the energy transfer mechanism in particular at large donor−acceptor distances. This can easily be understood by the following approximate picture. Let n be the number of donor molecules between a particular donor and an acceptor and r_{dd} be the distance between two donor molecules, so that $r = nr_{dd}$. An energy transfer mediated by sequential donor−donor transfer thus implies $k_{ET}(DD) \propto nr_{dd}^{-3}$, while a single-step Förster transfer over the same total distance r should follow $k_{ET}(PDA) \propto (nr_{dd})^{-6}$. Thus, single-step Förster-type donor−acceptor transfer can take over only at short distances due to a larger electronic coupling, while, at larger separations, sequential donor−donor transfer prevails.

The dominant contribution of exciton diffusion to the overall energy transfer from donor to acceptor has been recognized early in the literature. In fact, the role of a sequence of donor−donor transfers in moving excitation energy from one site to another has already been identified when investigating ordered dense media such as molecular crystals.[36,37] For disordered organic semiconductors, it was demonstrated that excitation energy transfer is to a large extent determined by the energy relaxation of excitons within an inhomogeneously broadened density of states distribution (spectral diffusion).[14,15,24,38] The relative contribution of energy migration within the polymer host to the overall energy transfer from the host to the dye guest has been investigated by Herz et al. in a time-resolved fashion.[13] They find exciton relaxation through incoherent hopping within the host's density of states controls the transfer dynamics in particular at short time scales up to a few tens of ps, while, at longer time scales, long-range single-step Förster transfer prevails. This is due to the fact that spectral diffusion is very fast at short time scales but then slows down as the excitons relax in the density of states distribution,[35] so that single-step Förster transfer becomes competitive. The inherent differences between excitation transfer through incoherent exciton hopping in films compared to solutions, and the anisotropy of this in polymer chains, have been addressed,[11,12] and sophisticated studies on exciton diffusion and its contribution to the overall energy transfer process are meanwhile available.[6−10]

Having confirmed that the dominant energy transfer mechanism here is sequential exciton hopping, we now consider the effects of oligomer length. Exciton hopping, i.e., excitation transfer from one donor molecule to its neighbor, is also mediated by dipole−dipole coupling, analogous to donor−acceptor transfer. The main difference pertains to the fact that the energy levels of two adjacent donor molecules differ only slightly due to energetic disorder, in contrast to the larger energy separation between levels of a donor and acceptor. This small difference and concomitantly small overlap between the emission of one donor molecule and the absorption of another donor molecule (Figure 2a) results in smaller transfer rates.

If we compare the experimental energy transfer rates found here for donor−acceptor blends made with the trimer, pentamer, and heptamer oligofluorenes as a function of center-to-center distance, we find an increase in overall transfer rate from trimer to pentamer blend but no further increase from pentamer to heptamer blend (Figure 5b). As the dominant transfer mechanism is donor−donor transfer, this difference must relate to an oligomer length dependence in the electronic donor−donor coupling. This is further supported by the fact that there is no significant difference in the energy transfer rates between the oligomers for a single-step donor−acceptor transfer, $k_{ET}(PDA)$,

where the changes in donor−acceptor overlap or donor lifetime are taken into account (Figure 5d). Thus, we consider the observed trend in donor−donor coupling must reflect the oligomer length dependence of the dipole−dipole coupling for a donor−donor pair.[39] In our work, we have experimentally found a maximum for the pentamer, i.e., for about 10 phenyl rings. This is large compared to the value of a maximum for about 3−4 phenyl rings calculated by Gierschner et al. for a cofacial pair of poly(para-phenylenes).[39] However, in the amorphous film, we consider an average coupling over many orientations and oligomer conformations; thus, a deviation from the value derived for an exactly cofacial pair is not surprising. In a way, this study on the dependence of the RET rate on oligomer length may be used as an experimental means to derive the maximum, ensemble averaged, electronic coupling.

CONCLUSIONS

We have investigated energy transfer from oligofluorene donors to an anthracene derivative acceptor as a function of oligomer length. We found the energy transfer to be dominated by exciton migration within the donor host. Consequently, the rate of energy transfer has been shown to be dependent on oligomer length insofar that it reflects the oligomer length dependence of the excitonic coupling between the donor host molecules. This is of particular importance for low acceptor concentrations and concomitant large donor−acceptor distances. When optimizing a host−guest system for energy transfer, it is therefore more important to match the host oligomer length to the maximum of its electronic coupling instead of optimizing the spectral overlap integral between donor and acceptor. We consider the oligomer length dependence of the RET rate may be employed as an experimental means to derive the oligomer length dependence of the ensemble averaged electronic coupling between the host molecules.

ASSOCIATED CONTENT

Supporting Information. Comparisons of the measurements carried out with the TCSPC setup and with the streak camera, thin film absorption spectrum of the anthracene derivative, parameters obtained by the stretched-exponential fits in Figure 4, time dependence of the RET rates, values for k_{ET}(EXP) and k_{ET}(PDA). This material is available free of charge via the Internet at http://pubs.acs.org.

AUTHOR INFORMATION

Corresponding Author

*E-mail: anna.koehler@uni-bayreuth.de (A.K.); rodrigo.albuquerque@uni-bayreuth.de (R.Q.A.).

ACKNOWLEDGMENT

R.Q.A. and A.K. are grateful for financial support from the GIF project (I-897-221.10/2005). J.K., R.Q.A., and A.K. would like to acknowledge financial support from the DFG project (GRK 1640).

REFERENCES

(1) Blom, P. W. M.; Vissenberg, M. C. J. M. *Mater. Sci. Eng., R* **2000**, *27*, 53.
(2) Hoppe, H.; Sariciftci, N. S. In *Photoresponsive Polymers II*; Marder, S.R., Lee, K. S., Eds.; Springer: Berlin, 2008; Vol. 214.
(3) Sun, Y. R.; Giebink, N. C.; Kanno, H.; Ma, B. W.; Thompson, M. E.; Forrest, S. R. *Nature* **2006**, *440*, 908.
(4) Chen, A. C. A.; Culligan, S. W.; Geng, Y. H.; Chen, S. H.; Klubek, K. P.; Vaeth, K. M.; Tang, C. W. *Adv. Mater.* **2004**, *16*, 783.
(5) Koeppe, R.; Sariciftci, N. S.; Buchtemann, A. *Appl. Phys. Lett.* **2007**, *90*, 181126.
(6) Madigan, C.; Bulovic, V. *Phys. Rev. Lett.* **2006**, *96*, 046404.
(7) Mikhnenko, O. V.; Cordella, F.; Sieval, A. B.; Hummelen, J. C.; Blom, P. W. M.; Loi, M. A. *J. Phys. Chem. B* **2008**, *112*, 11601.
(8) Athanasopoulos, S.; Hennebicq, E.; Beljonne, D.; Walker, A. B. *J. Phys. Chem. C* **2008**, *112*, 11532.
(9) Poulsen, L.; Jazdzyk, M.; Communal, J. E.; Sancho-Garcia, J. C.; Mura, A.; Bongiovanni, G.; Beljonne, D.; Cornil, J.; Hanack, M.; Egelhaaf, H. J.; Gierschner, J. *J. Am. Chem. Soc.* **2007**, *129*, 8585.
(10) Zapunidi, S. A.; Krylova, Y. V.; Paraschuk, D. Y. *Phys. Rev. B* **2009**, *79*, 205208.
(11) Dykstra, T. E.; Kovalevskij, V.; Yang, X. J.; Scholes, G. D. *Chem. Phys.* **2005**, *318*, 21.
(12) Markov, D. E.; Blom, P. W. M. *Phys. Rev. B* **2006**, *74*, 085206.
(13) Herz, L. M.; Silva, C.; Grimsdale, A. C.; Müllen, K.; Phillips, R. T. *Phys. Rev. B* **2004**, *70*, 165207.
(14) Movaghar, B.; Grunewald, M.; Ries, B.; Bässler, H.; Wurtz, D. *Phys. Rev. B* **1986**, *33*, 5545.
(15) Arkhipov, V. I.; Emelianova, E. V.; Bässler, H. *Phys. Rev. B* **2004**, *70*, 205205.
(16) Nguyen, T. Q.; Wu, J. J.; Doan, V.; Schwartz, B. J.; Tolbert, S. H. *Science* **2000**, *288*, 652.
(17) Schwartz, B. J. *Nat. Mater.* **2008**, *7*, 427.
(18) Huber, D. L. *Phys. Rev. B* **1979**, *20*, 2307.
(19) Förster, T. *Ann. Phys.* **1948**, *2*, 55.
(20) Beljonne, D.; Curutchet, C.; Scholes, G. D.; Silbey, R. J. *J. Phys. Chem. B* **2009**, *113*, 6583.
(21) Westenhoff, S.; Daniel, C.; Friend, R. H.; Silva, C.; Sundstrom, V.; Yartsev, A. *J. Chem. Phys.* **2005**, 122.
(22) Krueger, B. P.; Scholes, G. D.; Fleming, G. R. *J. Phys. Chem. B* **1998**, *102*, 5378.
(23) Beljonne, D.; Cornil, J.; Silbey, R.; Millie, P.; Bredas, J. L. *J. Chem. Phys.* **2000**, *112*, 4749.
(24) Scheidler, M.; Lemmer, U.; Kersting, R.; Karg, S.; Riess, W.; Cleve, B.; Mahrt, R. F.; Kurz, H.; Bässler, H.; Gobel, E. O.; Thomas, P. *Phys. Rev. B* **1996**, *54*, 5536.
(25) de Mello, J. C.; Wittmann, H. F.; Friend, R. H. *Adv. Mater.* **1997**, *9*, 230.
(26) Lieser, G.; Oda, M.; Miteva, T.; Meisel, A.; Nothofer, H.-G.; Scherf, U.; Neher, D. *Macromolecules* **2000**, *33*, 4490.
(27) Parkinson, P.; Aharon, E.; Chang, M. H.; Dosche, C.; Frey, G. L.; Köhler, A.; Herz, L. M. *Phys. Rev. B* **2007**, *75*, 165206.
(28) Wiesenhofer, H.; Beljonne, D.; Scholes, G. D.; Hennebicq, E.; Bredas, J. L.; Zojer, E. *Adv. Funct. Mater.* **2005**, *15*, 155.
(29) Munoz-Losa, A.; Curutchet, C.; Krueger, B. P.; Hartsell, L. R.; Mennucci, B. *Biophys. J.* **2009**, *96*, 4779.
(30) Khan, Y. R.; Dykstra, T. E.; Scholes, G. D. *Chem. Phys. Lett.* **2008**, *461*, 305.
(31) Steinberg, I. Z. *Annu. Rev. Biochem.* **1971**, *40*, 83.
(32) Calzaferri, G. *Top. Catal.* **2010**, *53*, 130.
(33) Koeppe, R.; Bossart, O.; Calzaferri, G.; Sariciftci, N. S. *Sol. Energy Mater. Sol. Cells* **2007**, *91*, 986.
(34) Cogdell, R. J.; Gall, A.; Köhler, J. *Q. Rev. Biophys.* **2006**, *39*, 227.
(35) Bässler, H. *Phys. Status Solidi B* **1993**, *175*, 15.
(36) Pope, M.; Swenberg, C. E. *Electronic Processes in Organic Crystals and Polymers*, 2nd ed.; Oxford University Press: Oxford, U.K., 1999.
(37) Benz, K. W.; Wolf, H. C. *Z. Naturforsch.* **1964**, *19a*, 177.
(38) Hildner, R.; Lemmer, U.; Scherf, U.; Köhler, J. *Chem. Phys. Lett.* **2006**, *429*, 103.
(39) Gierschner, J.; Huang, Y. S.; Van Averbeke, B.; Cornil, J.; Friend, R. H.; Beljonne, D. *J. Chem. Phys.* **2009**, *130*, 044105.